The Electrical Properties of the System $GdCo_{1-x}Fe_xO_3$ Synthesized by Chemical Route (x = 0.10, 0.20)

K.D. Mandal* and L. Behera

Department of Chemistry, North Eastern Regional Institute of Science and Technology, Nirjuli – 791109, Itaanagar, Arunachal Pradesh, India

ABSTRACT

The possibility of the formation of single phase in the system $GdCo_{1-x}Fe_xO_3$ was explored up to x = 0.20. A solid solution formed at low temperature using the chemical route for its synthesis. Single phase formation of prepared samples was confirmed by X-ray diffraction studies with a sharp distinguishing peak. The conduction occurs in the system by hopping of charge carriers as well as electrons for cobalt ions and holes for oxygen ions. Impedance studies explained the transport contribution in the system is due to its grains and grain boundaries.

Key words: Gadolinium cobaltate, perovskite oxide, chemical route, electrical conductivity, impedance study.

1. INTRODUCTION

The perovskite oxide is a field of great interest for material scientists. A number of perovskite oxides have been studied by various groups. We have been studying electrical and dielectric properties of perovskite oxide and valance compensated perovskite oxides $A_{1-x}M_xB_{1-x}N_xO_3$ which were synthesized by conventional ceramic methods. Recently we have taken up a few systems of perovskite oxides which were synthesized by the chemical route and published elsewhere /1-3/. Perovskite oxides have been studied extensively because of their technological applications, the reasons for which include their stability over wide temperature ranges, and their low cost. Composition and microstructure may be optimized and tailored to specific applications. Rare earth cobaltates show interesting electrical and magnetic properties. The properties of these materials depend on spin state and valance state of transition metal ions and ionic radii of rare earth ions.

* Corresponding author: E-mail address: kdm@nerist.ernet.in (K.D. Mandal)

In this paper we report the method of synthesis and characterization of the system $GdCo_{1-x}Fe_xO_3$ by studying electrical behaviour. We have tried to dope in B-site of $GdCoO_3$ by Fe ions which replaced Co ions proportionally. The change in electrical properties with doping of Fe^{+3} ions is also explained.

2. EXPERIMENTAL

Compositions with x = 0.10, 0.20, in the system $GdCo_{1-x}Fe_xO_3$, were prepared by the chemical method using citric acid. The chemicals used in this method have a purity of 99.9% or better. Gadolinium oxide, cobalt (II) nitrate and iron nitrate were used as starting materials.

Gadolinium oxide was converted into nitrate by adding conc. HNO_3 and evaporated to dryness. A standard solution of metal nitrate was prepared in distilled water. Solutions having a stoichiometric amount of these metallic ions in the system $GdCo_{1-x}Fe_xO_3$ (x = 0.10, 0.20) were mixed in a beaker. A calculated amount of citric acid, equivalent to the metal ions, was added to the solution. The solution was mixed on a hot-plate magnetic stirrer and warmed up to 60-70°C and the temperature was kept constant until total evaporation of water. The residue was dried at 50° - 60°C in a hot air oven. Dry powder was calcined at 600°C for 8 hrs. The calcined powder was ground into fine powder and made into cylindrical pellets. The pellets were sintered at 750°C for 6 hrs.

A thermo-gravimetric analysis (TGA) of the samples was carried out in a Delta Series TGA7 thermo-gravimetric analyzer. A sample (weighing 10-20 mg) was heated in nitrogen atmosphere at a rate of 10°C / minute and change of weight was recorded in the temperature range 30 - 830°C. The X-ray diffraction patterns of fine powder of the sintered pellets were recorded using Cu-K $_\alpha$ radiations. The DC electrical resistances of the sintered pellets coated with silver paint were measured with variation of temperature using a Keithley electrometer. The DC conductivity of the samples was calculated.

RESULTS AND DISCUSSION

All the compositions (x = 0.10, 0.20) synthesized in the system $GdCo_{1-x}Fe_xO_3$ were found to be single-phase materials. The crystal system, lattice parameter and unit cell volume for different compositions is calculated and given in Table 1. The recorded peaks were sharp and strong enough to confirm high crystallinity of the synthesized samples. The cell parameter and unit cell volume (V) increases with increase in Fe^{+3} ions concentration. This may be due to the large ionic radius of Fe^{+3} ion (0.78 Å) which, when substituted at B-site, displaces smaller /4/ Co^{+3} ions (0.66 Å). The unit cell volume for the system $GdCo_{1-x}Fe_xO_3$ having composition x = 0.20, increases about four times more than other samples, which may be due to low spin Co^{+3} converting to high spin Co^{+3} ions when iron content increases in the sample. Due to larger

Table 1

The crystal system, lattice parameter and unit cell volume for different compositions in the system $GdCo_{1-x}Fe_xO_3$

System	Value of (x)	Lattice System	Lattice Parameters			Unit Cell Volume (Å^3)
			a (Å)	b (Å)	c (Å)	
$GdCo_{1-x}Fe_xO_3$	0.10	Orthorhombic	5.2497	5.3064	7.5130	209.2882
$GdCo_{1-x}Fe_xO_3$	0.20	Orthorhombic	10.7338	7.4780	10.4144	835.9385

Fe^{+3} ionic radii, the unit cell volume of the orthorhombic structure converted into a pseudo-orthorhombic structure. The large unit cell contains a tetra-molecular orthorhombic unit.

Plots of log σ_{dc} vs 1000/T for various compositions in the system $GdCo_{1-x}Fe_xO_3$ are shown in Fig. 1. Intense peaks are observed for both the compositions x = 0.10 and 0.20 for the above system. Both the samples in the system $GdCo_{1-x}Fe_xO_3$ (x = 0.10, 0.20) under investigation show similar DC conductivity behavior. The insulator-metal transition occurred at temperatures of 393K and 465K for the compositions x = 0.10 and 0.20 respectively. The DC conductivity increased from room temperature to transition temperature for both systems, and then decreased with increase in temperature. The difference in transition temperature for the compositions x = 0.10 and 0.20 was found to be 72K. On increasing iron content in the above system, the transition temperature shifted to the higher temperature side (x = 0.20). The d-d coulomb interaction energy **U** and d-band width **w** dominated the electronic structure near the Fermi level. If **U** > **w** it is an insulator with a gap between the conductivity and valence bands determined by the energy required for fluctuations $2d \rightarrow d^{n+1} + d^{n-1}$. In the case of **U** < **w** it is a metal without a gap. From the experimental results it

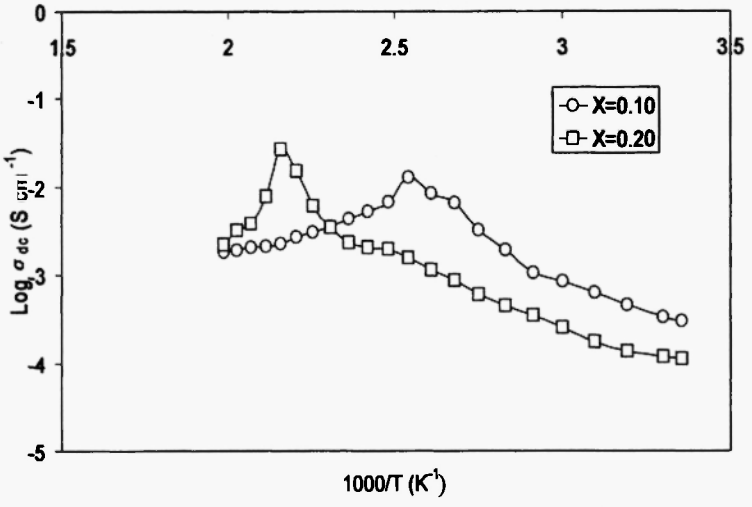

Fig. 1: Plots of log σ_{dc} vs 1000/T for the system $GdCo_{1-x}Fe_xO_3$ (x = 0.10, 0.20)

was found that $GdCoO_3$ is a so-called Mott insulator /5,6/. The conductivity observed in $GdCo_{1-x}Fe_xO_3$ may be due to Mobile holes created by excitation of an electron from the π^* band to an acceptor level. As the amount of Fe^{+2} in $GdCo_{1-x}Fe_xO_3$ substitution is increased, the acceptor orbital interacts to form an impurity band. If the high and low spin states have comparable energies, the formation of impurity bands generates a spontaneous ferromagnetism, wherein the σ^* bands of up-spin overlap the π^* band of downspin. The transport properties of $GdCo_{1-x}Fe_xO_3$ are explained by the complicated Co-3d band structure. The highest occupied molecular orbital contained Co-3d and O-2p orbitals. The insulator-metal transition, which appears at high temperatures, is not a Mott-Hubbard transition /7/ but a charge-transfer type transition. The spin state transition occurs mainly due to the variation of the Co-O bond length with increase of temperature. The transition occurs through the interaction between the 2p orbitals or the Co-3d and O-2p orbitals. $GdCo_{1-x}Fe_xO_3$ are nearly intermediate between Mott-Hubbard type compounds and charge transfer-type compounds with interaction between Co and O ions with valance and conductivity bands consisting of strongly mixed O-2p and Co-3d bands because of the electronic correlation. The covalence of $GdCo_{1-x}Fe_xO_3$ are due to the main contribution of the hybridization between Co and O orbitals. An increase of the Co-O bond length causes the low-spin state gradually to become unstable, while the high-spin state becomes stable. There is the possibility of the existence of an intermediate spin state. The insulator-metal transition occurs due to the interaction between mixed states consisting of electrons for Co ions and holes for O ions.

Plots of log σac vs 1000/T at 100Hz, 1kHz, 10kHz and 100kHz for the compositions x = 0.10, 0.20 in the system GdCo1-xFexO3 are shown in Fig. 2. The AC conductivity of the samples increased with temperature. It also seems from the figures that the nature of variation of AC conductivity with temperature is almost the same. In order to understand the mechanism of conduction, AC conductivity was measured as a function of frequency (100Hz – 5MHz) at three temperatures, 300, 350 and 400 K, which are shown in Fig. 3. It is noted that AC conductivity obeys the relation:

$$\sigma_{ac} = A\,\omega^s \qquad (1)$$

where $\omega = 2\pi f$ is the angular frequency and the exponent "s" is a weak function of frequency at a given temperature, A is a constant. The AC conductivity for both samples (x = 0.10, 0.20) of the $GdCo_{1-x}Fe_xO_3$ system increases with frequency at 300, 350 and 400 K. However, the nature of variation is different for different compositions. In general a large variation in AC conductivity is observed at low temperature and high frequency. AC conductivity for the composition x = 0.10 remains constant up to frequency 1, 10, 100 kHz at temperature 300, 350 and 400 K respectively. An interesting result is observed for the composition x = 0.20. AC conductivity for the composition x = 0.20 remains constant up to 10kHz below 400K. AC conductivity remains constant up to 10 and 100 kHz at 350 and 400 K respectively for the composition x = 0.10. The stability in AC conductivity, when frequency is higher at high temperatures, is observed for the composition x = 0.10. This shows that in the $GdCo_{1-x}Fe_xO_3$ system conduction occurs by excitation of charge carriers in the extended states above room temperature (350 and 400 K) up to 10kHz.

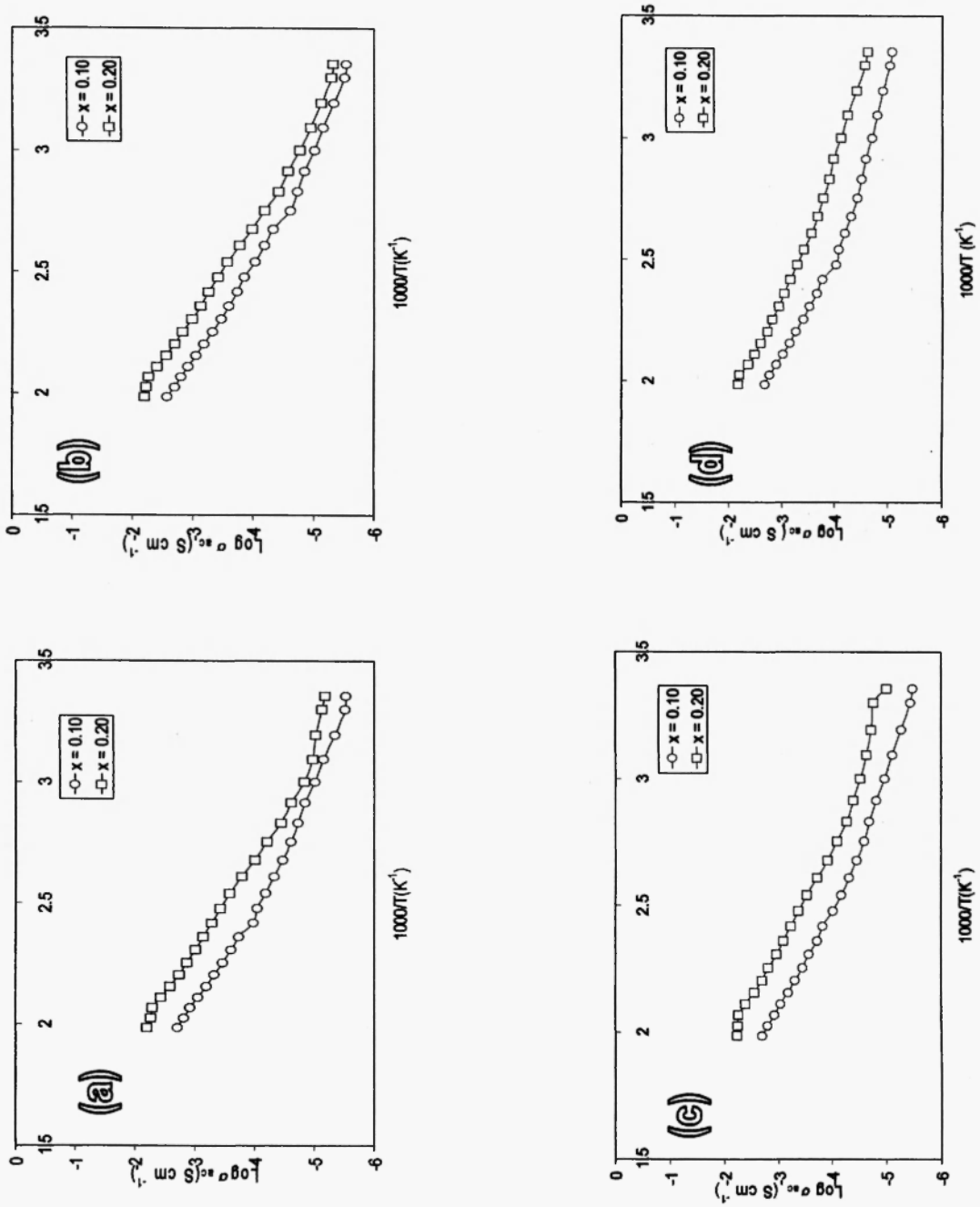

Fig. 2: Plots of log σ_{ac} vs 1000/T for the system $GdCo_{1-x}Fe_xO_3$ (x = 0.10, 0.20) at various frequencies (a) 100Hz, (b) 1kHz, (c) 10kHz, (d) 100kHz.

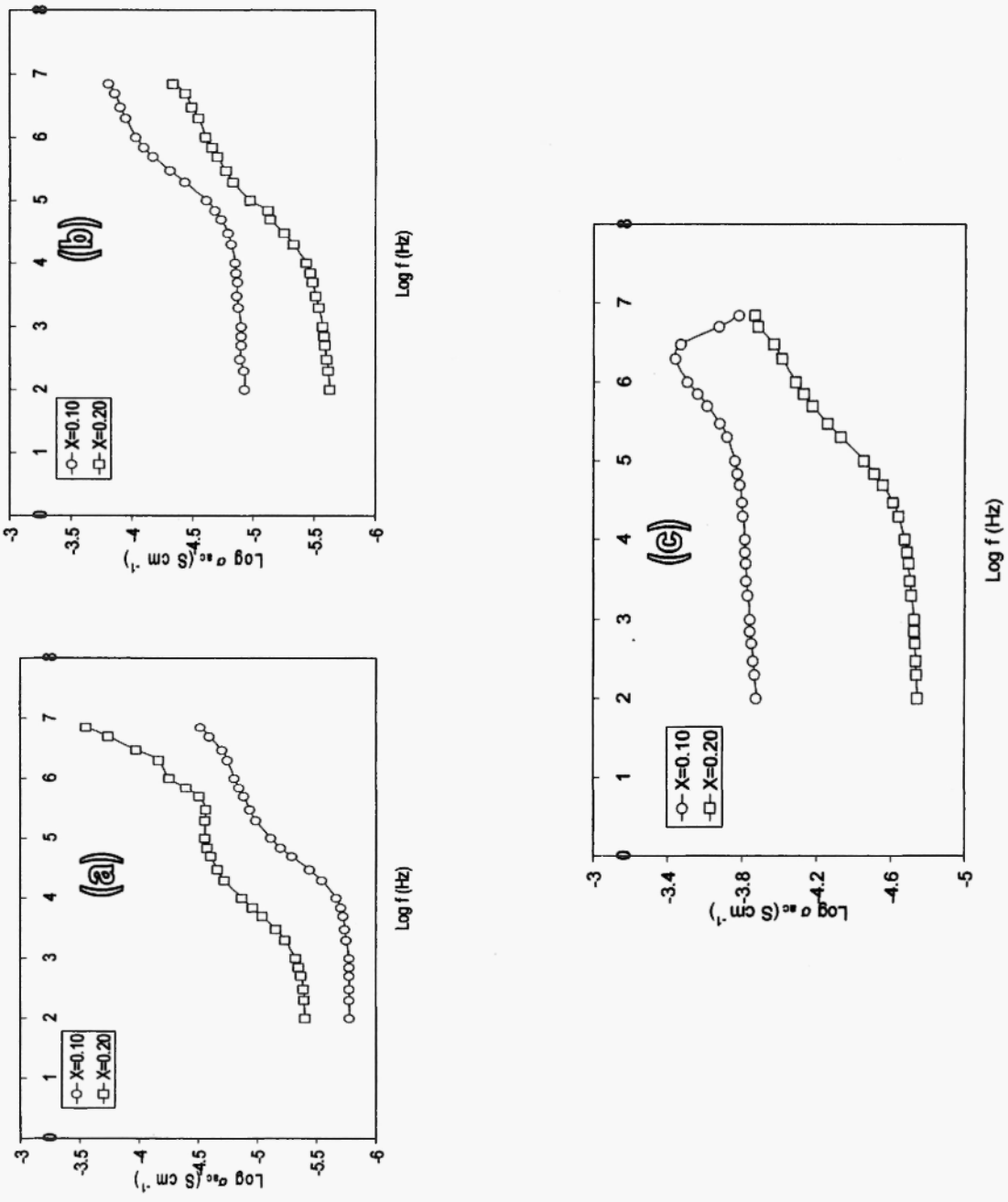

Fig. 3: Plots of log σ_{ac} vs log f for the system $GdCo_{1-x}Fe_xO_3$ (x = 0.10, 0.20) at various temperatures (a) 300 K, (b) 350 K, (c) 400 K.

The frequency dependence of AC conductivity may rise in the above composition due to the following mechanisms /8/:

i) Transport could take place by carriers excited into the localized states at the edges of valence or conduction band and hopping at the energies close to it.
ii) Hopping of charge carriers could occur in the localized states near the Fermi level.
iii) Hopping of the charge carriers among localized sites could give rise to a Debye-type loss similar to the thermally activated rotation of dipoles. These dipoles can point in two or more directions with different energies, w_1 and w_2 ($\Delta w = w_1 - w_2$) with a jump time (τ) from the lower to the upper states. Both Δw and τ vary over a wide range including zero.

The AC conductivity behavior of the system $GdCo_{1-x}Fe_xO_3$ with variation of temperature at different frequencies for the compositions x = 0.10 and 0.20 is similar, showing an increase with increase in temperature. The variation of log σ_{ac} conductivity with inverse of temperature for both compositions of the system $GdCo_{1-x}Fe_xO_3$ shows exponential dependence of AC conductivity, which shows that conduction in these samples occurs by mechanism iii). It is due to the excitation of charge carriers at the valence band edge and hopping at energies close to it. The values of AC and DC conductivities are shown in Table 2. It is found that activation energy for hopping increases with increases in x-value. This may be due to increasing disorder because of compositional fluctuations. These fluctuations are due to random occupation of octahedral sites by Fe^{+3} in the system $GdCo_{1-x}Fe_xO_3$.

Table 2

DC conductivity, activation energy, insulator-metal transition temperature and AC conductivity of the samples in the system $GdCo_{1-x}Fe_xO_3$.

System	Compositions (x)	DC conductivity at 400 K	Activation energy (eV)	Transition temperature (K)	AC conductivity at 400 K (100Hz)
$GdCo_{1-x}Fe_xO_3$	0.10	1.2735×10^{-2}	13.05×10^{-2}	393	1.3212×10^{-4}
	0.20	1.5498×10^{-3}	3.1559×10^{-2}	465	1.7864×10^{-5}

In these samples, the cobalt ions are predominantly in trivalent state. These materials also contain a small concentration of Co^{+2} ions. This is due to loss of oxygen during sintering /9/, the samples at higher temperature being converted according to the reaction:

$$O_o \rightarrow \frac{1}{2} O_2 + V_o + 2e^- \quad (2)$$

where all symbols used are from the Kroger-Vink notation of defects. The electron release in reaction (2) during the sintering process reduces Co^{3+} to Co^{2+} ions. The conduction is mainly due to the presence of

cobalt ions /10,11/ in these materials, as mentioned earlier. The AC conductivity that is almost frequency-independent (Fig. 3) up to a particular frequency at three different temperatures, 300K, 350K and 400K, for the compositions x = 0.10, 0.20 shows that conduction occurs by hopping of charge carriers among these localized sites according to mechanism iii).

The observed frequency-dependent AC conductivity in a certain frequency range also shows that there are two contributions to the observed AC conductivity: (i) due to conduction in the extended states which is frequency-independent, and (ii) due to hopping among localized sites which is frequency-dependent, which may be variable in nature. The second contribution varies according to Equation (2). The value of "s" is found to be negative in the system $GdCo_{1-x}Fe_xO_3$ (x = 0.10, 0.20) at high frequency.

4. IMPEDANCE STUDIES

Impedance spectroscopy is a relatively new and powerful analytical method, playing an important role in material science for characterization of electrical properties of materials and their interfaces with electronically conducting electrodes /12-15/. It is used to investigate the dynamics of bound or mobile charges in bulk or interfacial regions of any kind of solid or liquid materials, ionic /16/, mixed conductors, semiconductors and even dielectrics.

Impedance is a complex quantity defined as:

$$Z^*(\omega) = Z'(\omega) - iZ''(\omega) \tag{3}$$

where $Z'(\omega)$ is a real part and $Z''(\omega)$ is an imaginary part of the total impedance which is calculated from Equations (4 and 5), i is an imaginary number = $\sqrt{-1} = \exp(\pi i)/2$, indicating an anticlockwise rotation by $\pi/2$ relative to the X-axis in the X-Y plane.

$$Z' = G/\left(G^2 + \omega^2 C^2\right) \tag{4}$$

$$Z'' = \omega C/\left(G^2 + \omega^2 C^2\right) \tag{5}$$

where G is conductance, C is the capacitance, and $\omega = 2\pi f$ is the angular frequency. The impedance spectroscopy or complex plane analysis method is based on the measurement of variation of the cell impedance with frequency. In measurements, the measured response is frequency-dependent and contains contributions from the whole cell. The charge transport through this polycrystalline sample-electrode assembly involves three processes: (i) bulk or lattice conduction, (ii) grain boundary conduction, and (iii) transport across the electrode sample interface or electrode polarization. The whole charge transport process is in principle represented by an analogous electrical circuit (Fig. 4), which is a series combination of three

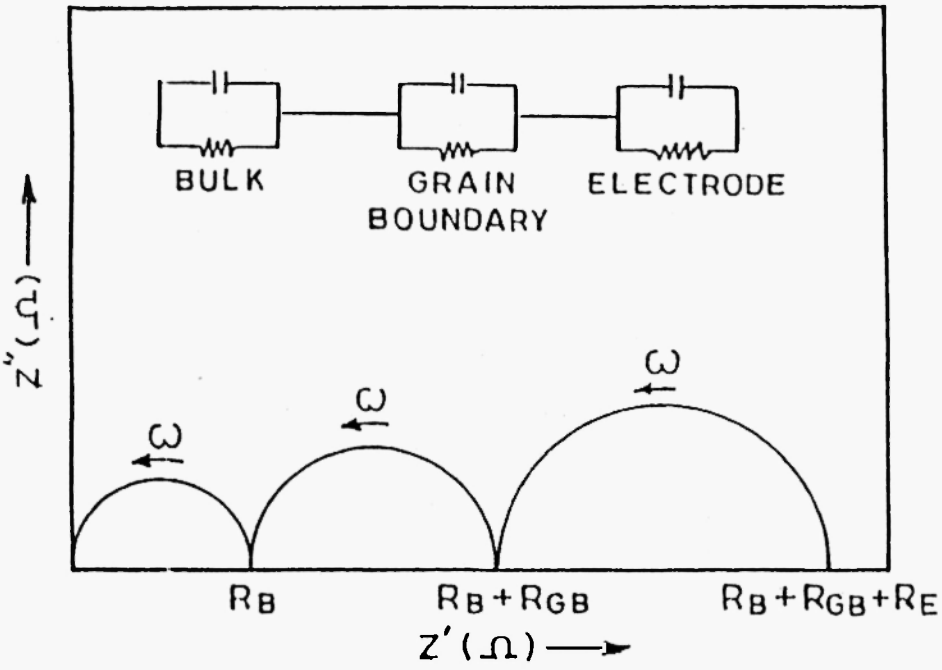

Fig. 4: Schematic representation of equivalent circuit and the corresponding impedance plots for the electrical transport through a polycrystalline material.

R-C (Resistance-Capacitance) parallel networks. Generally, the highest frequency arc represents the bulk resistance, the intermediate frequency arc represents the grain boundary resistance and the lowest frequency arc represents the contribution of the electrode process to the total observed resistance. The resistance values of the three contributions are obtained from the intercept of the circular arc with the real axis /17/.

In this paper, we have used impedance spectroscopy for separating various contributions to the total observed resistance to study the mechanism of conduction in B site substituted perovskite oxide systems:

i) The contribution from grains known as inter-granular or bulk conduction, designated by $-G_b$;
ii) The contribution from the grain boundaries, designated as $-G_{gb}$;
iii) The contribution from the solid-electrode interfaces, known as $-G_{el}$.

The corresponding resistance is represented by R_b, R_{gb} and R_{el}. Each of these contributions can be represented by a suitable combination of resistance and capacitance in parallel. The typical impedance plots Z'' vs Z' for these samples (x = 0.10, 0.20) in $GdCo_{1-x}Fe_xO_3$ are shown in Figs. 5 and 6 at three temperatures (300, 350 and 400 K). For the sample x = 0.10 in the $GdCo_{1-x}Fe_xO_3$ system, two semicircular arcs with the center on the Z' axis are observed at 300K and 350K but only one depressed semicircular arc is observed at 400K, which is not passing through the origin (Fig. 5 (c)). But the sample x = 20 gives two semicircular arcs at 300, 350 and 400 K (Figs. 6 (a), (b), (c)). The resistance for grains and grain-boundaries for different

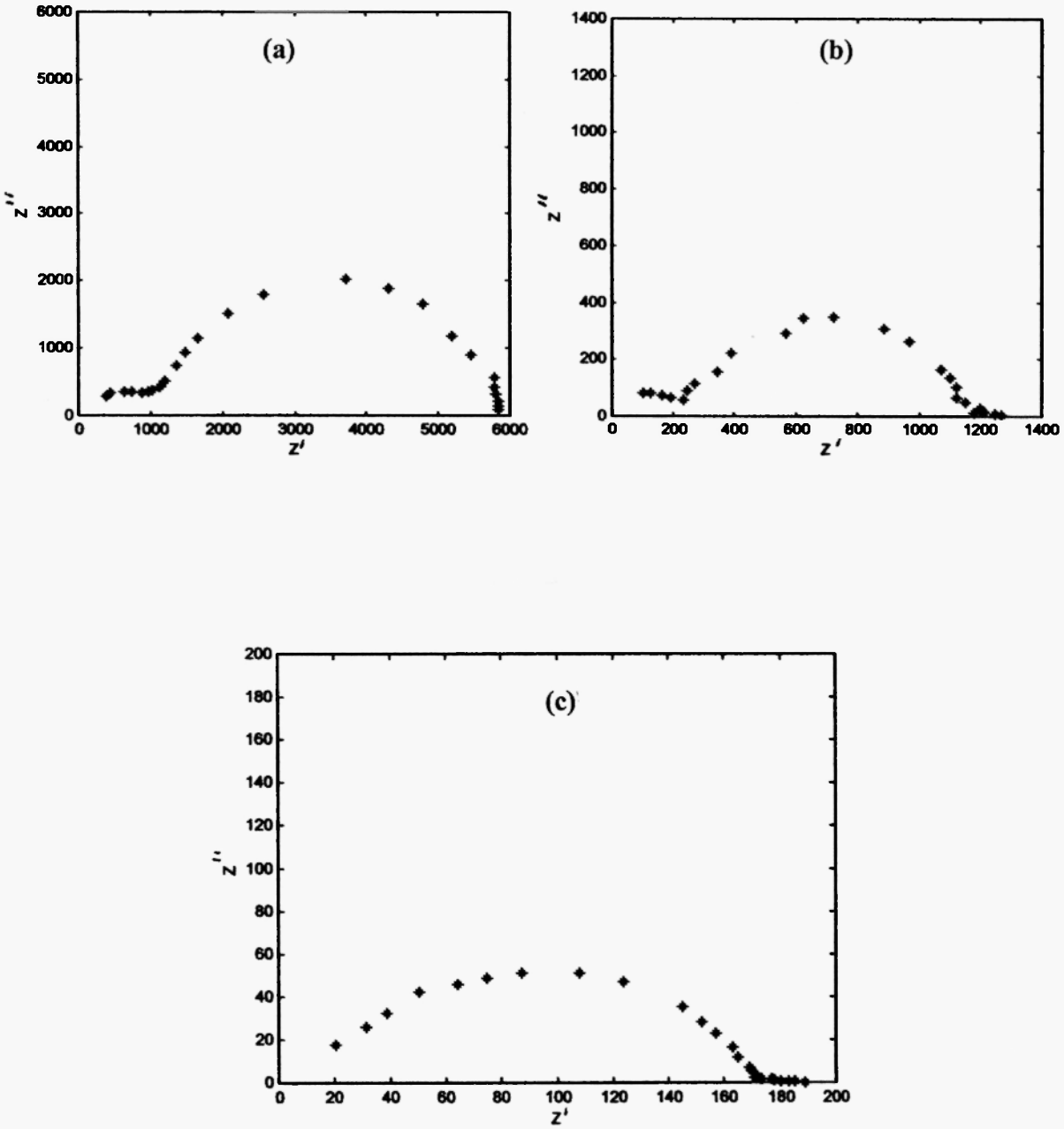

Fig. 5: Impedance plots of $GdCo_{0.9}Fe_{0.1}O_3$ at (a) 300 K, (b) 350 K and (c) 400 K.

samples was calculated with the help of these plots, and is given in Table 3. The size of the semicircles is different for grains and grain-boundaries, which indicates that they have different resistance values. It is also observed that the size of the semicircular arc changes with temperature variation. Only one semicircular arc is observed (Fig. 5 (c)), due to large resistance differences caused by temperature variation in $GdCo_{1-x}Fe_xO_3$

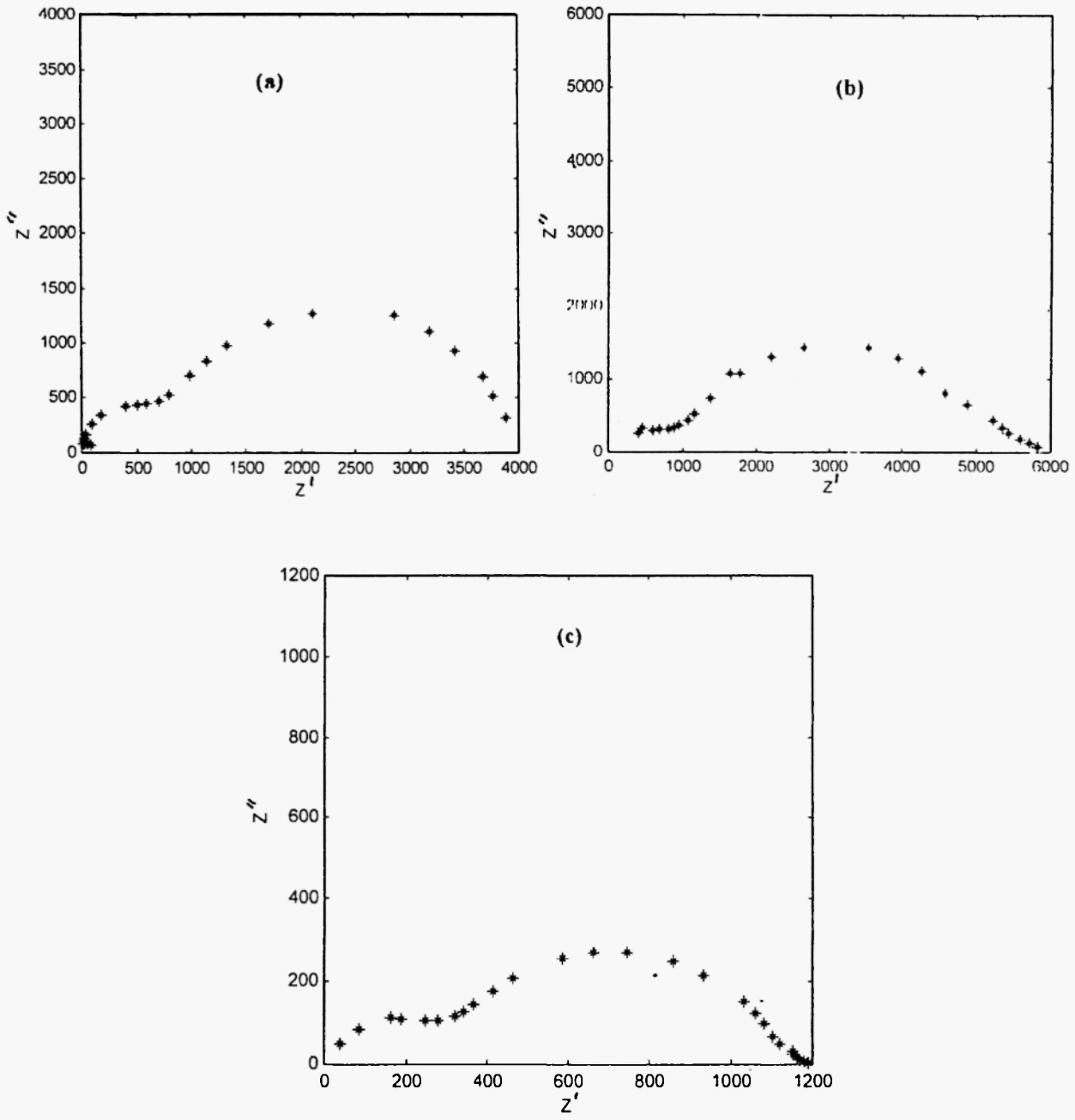

Fig. 6: Impedance plots of $GdCo_{0.8}Fe_{0.2}O_2$ at (a) 300 K, (b) 350 K and (c) 400 K.

(x = 0.10). The resistance of the grain boundaries seems to be very high in these samples, as indicated by a very wide circular arc in the low temperature region. The grain boundaries at low temperature behave as pure capacitive elements. As the temperature increases, the resistance of the grain boundaries decreases, and this gives rise to two distinct circular arcs at higher temperatures in the impedance plots. Below this temperature

only one semicircular arc is observed, which is due to large differences in R_b and R_{gb}. The complex impedance plots of this composition 0.10 (Fig. 5 (c)) show only one circular arc over the frequency range 100Hz – 5MHz, indicating that the grain boundaries are not behaving differently from the bulk. The electrical transport is mainly due to the contribution of bulk and grain boundaries. The semicircular arc with higher frequency range passing through the origin represents the bulk contribution due to grains, while the other, in the low frequency range, corresponds to the grain boundary contribution to the total observed resistance. There is no significant contribution from the electrode process as, during the measurement, dc conductivity was found to be independent of time, indicating the absence of any electrode polarization.

Table 3

Resistance of grains and grain-boundaries for the system $GdCo_{1-x}Fe_xO_3$ at different temperatures

System	Composition	Temperature 300 K		Temperature 350 K		Temperature 400 K	
		R_b (Ω)	R_{gb} (Ω)	R_b (Ω)	R_{gb} (Ω)	R_b (Ω)	R_{gb} (Ω)
$GdCo_{1-x}Fe_xO_3$	x = 0.10	1000	4916	260	940	168	–
	x = 0.20	1000	3050	1000	4642	333	799

The big arc is due to the grain boundary contribution and this may be due to the high value of resistance at lower frequencies. The small arc is due to the bulk contribution, active during the transport process, because it offers less resistance at higher frequencies. In these plots there is no third semicircular arc. Hence there is no significant contribution of charge transport through the electrode-sample interface due to very good contact of silver paint used on the sample surface. At 300K and 350K temperatures the grain boundaries are more resistant as compared to the bulk of the sample. This confirms the formation of barrier layers in these materials. In the case of 400K, however, we observed one arc at higher frequencies, also at higher temperature. This may be due to the transport contribution occurring only because of the bulk of the materials. This, indicating that the circuit contains two components and is capable of representing a single relaxation process, can be expressed as a series or a parallel combination /18/.

ACKNOWLEDGEMENT

The authors are grateful to the Council of Scientific and Industrial Research, New Delhi, for financial assistance.

REFERENCES

1. K.D. Mandal and Om Parkash, *Cryst. Res. Technol.*, **31** (3), K36-K39 (1996).
2. K.D. Mandal, L. Behera and K. Ismail, *Journal of Alloys and Compounds*, **352**, 309-314 (2003).
3. K.D. Mandal, L. Behera and R.C. Behera, *Journal of Materials Science and Technology*, **10**, 4 (2002).
4. R.D. Shannon and C.T. Prewett, *Acta Crystallogr.*, **B26**, 1046 (1970).
5. N.F. Mott, *Proc. Roy. Soc. London, Ser. A*, **62**, 416 (1963).
6. N.F. Mott, *Metal-Insulator Transitions*, Taylor & Francis, London, 1990.
7. J. Hubbard, *Proc. Roy. Soc. London, Ser. A*, **276**, 238 (1963).
8. N.F. Mott and E.A. Davis, *Electronic Process in Non-Crystalline Materials*, Clarendon, Oxford, 1979; Chap. 6.
9. I. Burn and S. Neirman, *J. Mater. Sci.*, **17**, 3510 (1982).
10. C.N.R. Rao, V.G. Bhide and N.F. Mott, *Philos. Mag.*, **32**, 1277 (1975).
11. P.M. Raccah and J.B. Goodenough, *J. Appl. Phys.*, **39**, 1209 (1968).
12. J.F. Bauerle, *J. Phys. Chem. Solids*, **30**, 2657 (1969).
13. J.R. Macdonald, *J. Chem. Phys.*, **61**, 3977 (1974).
14. A.D. Franklyn, *J. Am. Ceram. Soc.*, **58**, 465 (1975).
15. I.M. Hodge, M.D. Ingram and A.R. West, *J. Electroanal. Chem.*, **74**, 125 (1976).
16. A. Hooper, *J. Phys. D.*, **10**, 1487 (1977).
17. H.S. Maiti and R.N. Basu, *Mater. Res. Bull.*, **21**, 1107 (1987).
18. O. Prakash, L. Panday, H.S. Tewari, V.B., Tare and D. Kumar, *Ferroelectric*, **102**, 203 (1990).